

To be submitted to
Physical Review B

ISTITUTO NAZIONALE DI FISICA NUCLEARE
Laboratori Nazionali di Frascati

LNF-84/42(P)
20 Giugno 1984

A.Balerna, E.Bernieri, P.Picozzi, A.Reale, S.Santucci, E.Burattini
and S.Mobilio : AN EXAFS AND XANES STUDY ON
EVAPORATED SMALL CLUSTERS OF Au

AN EXAFS AND XANES STUDY ON EVAPORATED SMALL CLUSTERS OF Au

A. Balerna, E. Bernieri, P. Picozzi, A. Reale, S. Santucci
Istituto di Fisica dell'Università de L'Aquila

E. Burattini
CNR and INFN-Laboratori Nazionali di Frascati

and

S. Mobilio
INFN-Laboratori Nazionali di Frascati

ABSTRACT

Gold evaporated small metal clusters have been studied by X-ray absorption spectroscopy on the L_3 Au edge at the Frascati synchrotron radiation facility. Sample discontinuity and particle size were controlled by optical transmission measurements and electron microscopy analysis. The EXAFS spectra showed the presence of nearest neighbour distance contraction, whose value reached 2.5% for the smallest clusters. The behaviour of the nearest neighbour distance contraction versus cluster diameter agreed with a macroscopic liquid drop model. Increases of the nearest neighbour distance fluctuations around the equilibrium positions were found, due to the higher mobility of the surface atoms with respect to the bulk ones. The slight increase of statical disorder together with the general features of the XANES spectra allowed us to exclude structural changes from the fcc bulk metal structure, to the icosahedral structure even for 200 atoms cluster.

1. - INTRODUCTION

During the last decade, the chemical and physical properties of small metal clusters have been an active area of research⁽¹⁻¹⁶⁾. In fact the enhancement of chemical reactivity⁽¹⁷⁾, the lowering of the melting temperature⁽¹⁸⁾ and the magnetic behaviour^(19,20) of the metal clusters are peculiar properties largely used in many technological applications, among which heterogeneous catalysis⁽¹⁷⁾. Many theoretical and experimental studies have been and are being performed on the electronic and structural properties of metal clusters in different conditions such as chemical environment, sample preparation, size and substrates^(1-17,21-27). Many problems are still unsolved: for instance it is not known if the cluster, size dependent, chemical reactivity is due to a change in their electronic or in their structural properties and how these properties depend on the samples preparation method and on the interaction with substrates^(1,17).

In this paper we report an investigation on the structural properties of Au clusters, evaporated on a weakly interacting substrate, whose average diameters range from 11 Å up to 60 Å.

In the past, experiments, using diffraction, have been made on Au clusters in order to measure the lattice parameters as a function of the cluster size^(28,29). Lattice parameter contractions have been observed, but there is a great disagreement among the numerical values obtained on clusters of same diameter: for instance for a 35 Å cluster diameter values ranging from 0.4% to 2.7% are reported. This is due to the diffraction method which becomes less and less sensitive as the cluster size decreases⁽³⁰⁾.

In order to determine the effective amount of contractions and to check also changes in the crystallographic cluster structure^(31,32), we performed a complete structural investigation using EXAFS^(33,34) (Extended X-ray Absorption Fine Structure) and XANES^(35,36) (X-ray Absorption Near Edge Structure).

The layout of this paper is as follows: in Sect. 2. we report the sample preparation; we briefly describe the details regarding their characterization using optical transmittance and electron microscopy measurements and describe the X-ray absorption spectra. Sect. 3. contains the X-ray absorption and EXAFS data analysis. In Sect. 4. there is the discussion of the results and their interpretation. Sect. 5. is a summary of the main results.

2. - SAMPLE PREPARATION AND CHARACTERIZATION; ABSORPTION MEASUREMENTS.

Cluster samples were prepared under vacuum on a 6 μm polymer film by consecutive evaporations of gold (purity=99.99%) and mylar to achieve the optimum metal thickness for X-ray measurements⁽³³⁾. The amount of Au deposited on each layer of the different samples studied, is reported in Table I; mylar thickness was always around 200 \AA . Gold and mylar depositions were both controlled with a quartz-crystal detector.

TABLE I - Values of coverages (t), mean diameters (D) and diameter standard deviations (σ) of the samples studied.

t (atoms/cm ²)	D (\AA)	σ (\AA)
0.6×10^{15}	11.0	6.5
1.8×10^{15}	15.0	5.4
3.0×10^{15}	20.0	7.5
4.1×10^{15}	24.0	8.2
5.9×10^{15}	30.0	8.9
12.0×10^{15}	42.5	11.0
18.0×10^{15}	60.0	18.0

In order to check that the multilayer samples were discontinuous, optical transmission measurements have been made at normal incidence in the spectral range 0.25-2.5 μm . It is known that transmittance spectra of discontinuous films, contrary to continuous films spectra, generally show a wide minimum (Optical Conduction Resonance) below the interband transitions⁽³⁷⁾ due to the free electrons in the metal particles and an high transmission in the near IR⁽³⁸⁾. The comparison between the optical transmission spectra of our samples and of a continuous film demonstrates the sample discontinuity (Fig. 1).

The distributions of clusters dimensions have been determined by electron microscopy analysis (Fig. 2 and Table I).

X-ray absorption spectra (Fig.3) at liquid nitrogen temperature (LNT) and at room temperature (RT) have been recorded on the L_3 Au absorption edge at the Frascati National Laboratory using the wiggler photon beam line, with typically $I=40$ mA and $E=1.5$ GeV in the storage ring and $B=18.5$ kG in the wiggler magnet^(39,40). The critical energy, in this condition, is 2.77 keV. The monochromator was equipped with a Si(111) channel-cut crystal and the detection of the X-ray beam was achieved by two ionization chambers filled with Kr gas.

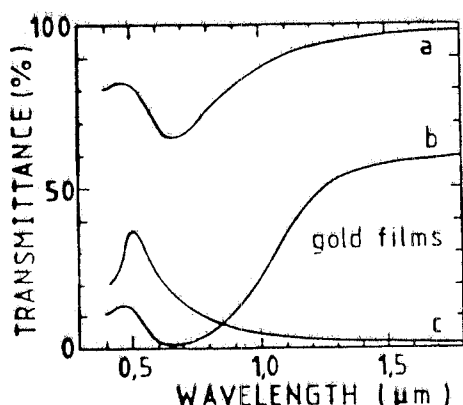


FIG. 1 - Example of comparison between measured optical transmittance spectra of different gold films; a) single discontinuous layer with a coverage of 18.0×10^{15} atoms/cm², b) 10 discontinuous layers having each a coverage of 18.0×10^{15} atoms/cm², and c) continuous film having the same total thickness of sample b).

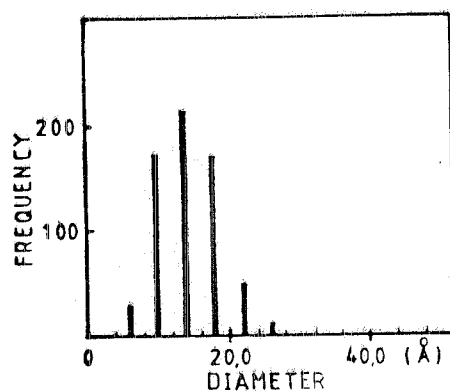
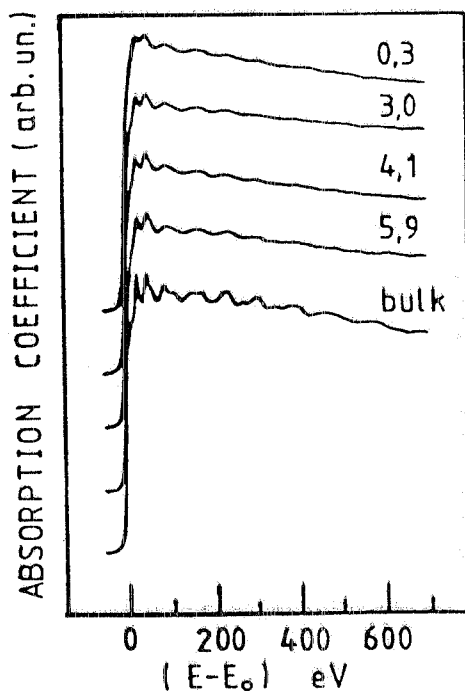


FIG. 2 - Gold cluster size distribution for a coverage of 1.77×10^{15} atoms/cm².

FIG. 3 - Absorption coefficients at the L_3 Au edge of some of the samples studied. Coverages indicated in the figure for each sample are in units of 10^{15} atoms/cm². The zero of the energy has been assumed at the edge inflection point.



3. - EXAFS DATA ANALYSIS

X-ray absorption spectra have been analyzed using a standard procedure⁽⁴¹⁾ to extract the oscillating part of the spectrum, or $\chi(k)$, given by⁽³⁴⁾:

$$\chi(k) = \frac{\mu_{L_3}(k) - \mu_0(k)}{\mu_0(k)}$$

where $\mu_{L_3}(k)$ is the Au L_3 -shell contribution to the absorption coefficient, $\mu_0(k)$ is the atomic absorption coefficient about which $\mu_{L_3}(k)$ oscillates and k is the photoelectron wavevector given by:

$$k = \left[\frac{2m(E - E_0)}{h^2} \right]^{1/2}$$

where E is the incoming photon energy and E_0 is the threshold energy.

In general, there are two contributions to an L_3 edge, coming from two possible transitions: $2p_{3/2}$ and $2p_{1/2}$. It has been theoretically demonstrated and experimentally proved⁽⁴²⁻⁴⁴⁾ that the former is only a few percent of the latter. As a consequence the EXAFS on an L_3 edge can be well approximated by the single final state expression of a K edge⁽³³⁾:

$$\chi(k) = \sum_j \frac{S_0^2 N_j |f_j(k, \pi)| e^{-2k^2 \sigma_j^2}}{k R_j^2} \sin(2k R_j + \Phi_j^{L_3}) \quad (1)$$

In relation (1), R_j is the distance between the absorbing and backscattering atom, N_j is the number of the backscattering atoms in the j -th shell, σ_j^2 is the mean square fluctuation in R_j , $|f_j(k, \pi)|$ is the backscattering amplitude of the neighboring atoms, $\Phi_j^{L_3}(k)$ is the k dependent phase shift for d -symmetry final state and S_0^2 is the reduction factor due to multielectron excitation. Informations on the structural parameters R_j , σ_j^2 and N_j can be obtained from EXAFS spectra if the scattering functions $|f_j(k, \pi)|$ and $\Phi_j^{L_3}(k)$ are known. These functions can be transferred, from a system to another one, provided that the two systems are chemically similar^(45,46).

Gold phase and backscattering amplitude have been obtained analysing the EXAFS spectrum of a 4 μ m Au foil at LNT (Fig. 4a). The Fourier Transform (FT) of this EXAFS spectrum (Fig. 4b) shows several peaks, corresponding to the different coordination shells shifted from the crystallographic values by a quantity due to the presence of the phase term in $\chi(k)^{(47)}$. We note that the first peak in real space is splitted, due to the Au highly non linear phase (Fig. 5a) and to the oscillatory behavior of the backscattering amplitude (Fig. 5b). The positions and relative intensities of these two splitted components depend on the FT conditions as can be seen comparing the bulk FT of Fig. 4b and Fig. 6. For this reason we transformed all the clusters EXAFS spectra under the same conditions (Fig. 6).

It is evident that as the film thickness decreases there is a shift of the FT main peak towards smaller R. Table II reports the nearest neighbour (nn) distance values obtained.

Informations about the mean coordination numbers and the Debye-Waller factors were obtained from data analysis in k-space. The inverse Fourier transform of the first FT double peak, allows to select the contribution to the $\chi(k)$ due only to the first coordination shell. In this way it is possible to analyze separately the amplitude function:

$$A(k) = \frac{S_0^2 N}{R^2} e^{-2k^2 \sigma^2} |f(k, \pi)|$$

and the "total" phase function⁽⁴⁸⁾:

$$\Pi(k) = 2kR + \Phi^{L^3}$$

Plotting the function

$$\ln \left(\frac{A_{cluster}}{A_{bulk}} \right)$$

versus k^2 , a straight line is obtained⁽⁴⁸⁾ whose slope is given by:

$$-2(\sigma_{cluster}^2 - \sigma_{bulk}^2)$$

and whose extrapolation to $k^2=0$ is

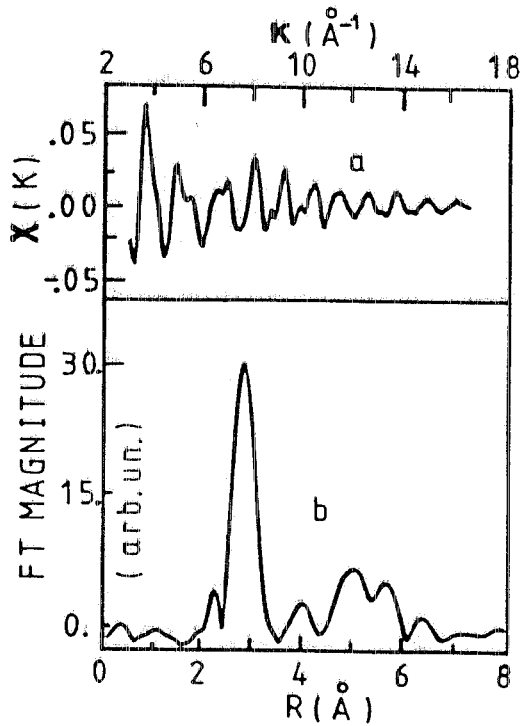


FIG. 4 - a) EXAFS spectrum of Au Bulk at 77K; b) Fourier transform of bulk EXAFS spectrum k in the range $3-16 \text{ \AA}^{-1}$ with a gaussian window function and a k^3 weight.

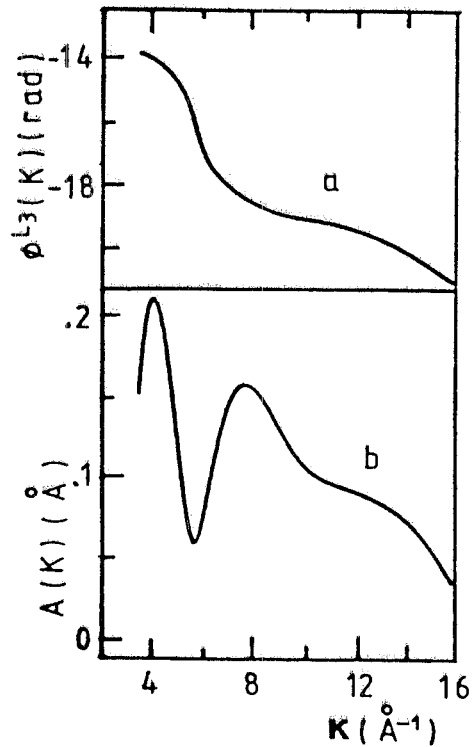


FIG. 5 - Phase (a) and amplitude (b) functions for Au bulk at 77K, obtained backtransforming the region $2.1-3.5 \text{ \AA}$ of Fig. 4b.

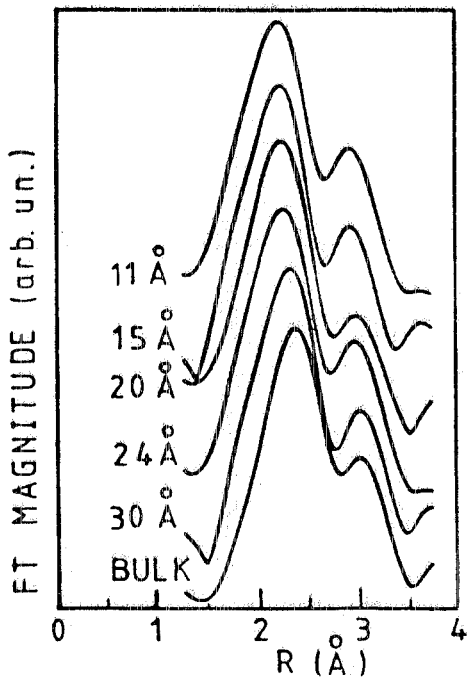


FIG. 6 - Fourier transforms of the films and bulk EXAFS spectra. The transformations are now in the range $3-11 \text{ \AA}^{-1}$ with k^1 weight and a gaussian window function.

TABLE II - Values of the nearest neighbour distances of Au clusters obtained from Fourier spectra and from k -space analysis. The Fourier values have been obtained adding the phase shift contribution $\delta = 0.51 \text{ \AA}$, calculated from the bulk spectrum, to the positions of samples Fourier spectra maxima.

$D(\text{\AA})$	$R_{\text{FOURIER}}(\text{\AA})$ $\pm 0.02 \text{ \AA}$	$R(k)(\text{\AA})$ $\pm 0.01 \text{ \AA}$
11.0	2.82	2.81
15.0	2.83	2.82
20.0	2.84	2.83
24.0	2.85	2.85
30.0	2.86	2.85
42.5	2.87	2.86
60.0	2.87	2.87

$$\ln \frac{\left(\frac{N}{R^2}\right)_{cluster}}{\left(\frac{N}{R^2}\right)_{bulk}}$$

The values of N and σ^2 obtained, using this approach, are reported in Table III. We note that as the cluster size decreases the mean coordination number decreases and the cluster disorder factor increases.

TABLE III - Coordination numbers (N) and Debye-Waller factors (σ^2) at 300K and 77 K obtained from analysis in k-space. The bulk σ_B^2 at 77 K has been assumed equal to $1.7 \times 10^{-3} \text{ \AA}^2$ according to Ref. (59).

D(Å)	N (±10%)	$\sigma_{300K}^2 (\text{Å}^2)$ (±20%)	$\sigma_{77K}^2 (\text{Å}^2)$ (±20%)
BULK	12.0	4.9×10^{-3}	1.7×10^{-3}
42.5	11.0	6.7×10^{-3}	2.4×10^{-3}
30.0	10.6	7.0×10^{-3}	2.6×10^{-3}
24.0	10.0	8.6×10^{-3}	4.2×10^{-3}
20.0	9.6	10.7×10^{-3}	5.5×10^{-3}
15.0	9.4	10.0×10^{-3}	----

It is also possible to obtain the nn distances in the k-space⁽⁴⁹⁾, using the following relation:

$$R_{cluster} = \frac{\Pi_{cluster}(k) - \Phi^{Ls}(k)}{2k}$$

The values so obtained are just like the ones obtained in the R-space (Table II).

Great attention was given to the possible presence of asymmetry effects in the radial distribution function (RDF), which can result in apparent nn contractions⁽⁵⁰⁾. The origin of such effects can be dynamical or static⁽⁵¹⁻⁵³⁾. We can exclude the presence of dynamical asymmetry effects because the cluster total phase obtained by EXAFS data analysis was found to be independent from temperature. Besides the asymmetry effects on Pt/SiO₂ clusters have been experienced negligible up to 500 K⁽⁵⁴⁾.

Presence of asymmetry static effects can be excluded "a posteriori" since the analysis with a gaussian function gives a decrease in the nn distances, a decrease of the coordination numbers and an increase of the Debye-Waller factors which are completely explained by the increased surface to volume ratio.

4. - DISCUSSION

4.1. - Interatomic Distances Results

Fig. 7 shows the nn distance contractions found as a function of the inverse of mean cluster diameter. These values clearly proof a contraction in the nn distances up to 2.5%. We believe that these results obtained by EXAFS have not the same kind of limitations that diffraction results have. EXAFS in fact is able to measure also a dimer interatomic distance⁽¹⁶⁾. From a macroscopic point of view the contraction of the nn distances is explained in terms of surface stress due to the high value of the surface to volume ratio in the clusters. For a liquid drop model⁽⁵⁵⁾, the contraction ΔR due to surface stress (f) is given by:

$$\Delta R = -\frac{4}{3}KR_b f \frac{1}{D}$$

where K is the bulk compressibility, R_b is the metal bulk nn distance and D is the mean cluster diameter. Data in Fig. 7 clearly show a linear dependence versus $1/D$. From this analysis we argue that the macroscopic approximation is surely valid for cluster size greater than 11 Å.

Our results are in contrast with recent EXAFS results on metal clusters in catalytic systems where the nn distances are similar to the bulk ones within 0.02 Å^(12-14,56). On the other hand they agree with those on Cu and Ni clusters prepared under vacuum evaporation^(15,24). These two different behaviours are due to the different metal-substrate interactions. It has been experimentally demonstrated that when there are no interactions between metals and substrates, as in the case of metal clusters in rare gas matrices, contractions are present^(16,57). In our case the interactions between clusters and substrates are certainly weak, as will be shown in what follows.

4.2. - Coordination Numbers Results

Fig. 8 shows the experimental behavior of the mean coordination number reported by Mason⁽¹⁾ for gold on carbon versus coverage together with our EXAFS results. We want to stress that our data are the first direct determination of coordination numbers in evaporated metal clusters. The agreement observed, demonstrates that mylar, like carbon, is a weakly interacting substrate for metal clusters and states again that there are no asymmetry effects. In fact another main effect of an asymmetric RDF is a dramatic lowering of the coordination numbers⁽⁵⁰⁾.

4.3. - Debye-Waller Factors Results

The increase in cluster disorder is mainly dynamical in the origin. The behavior of σ^2 versus T^2 is reported in Fig. 9. In the Debye correlated approximation⁽⁵⁸⁾

$$\sigma^2(T) = \sigma_S^2 + \frac{6\hbar^2}{mk_B\Theta_D} \left[\frac{1}{4} + \left(\frac{T}{\Theta_D} \right)^2 D_1 \right] - \frac{6\hbar^2}{mk_B\Theta_D} \left[\frac{1 - \cos(q_D R_j)}{2(q_D R_j)^2} + \left(\frac{T}{\Theta_D} \right)^2 D_1 \right] \quad (2)$$

where σ_S^2 is the static contribution to the disorder, Θ_D and q_D respectively are the Debye temperature and wavevector and k_B is the Boltzmann constant; D_1 is the slowly varying function:

$$D_1\left(\frac{\Theta_D}{T}\right) = \int_0^{\Theta_D/T} \frac{x}{e^x - 1} dx.$$

The use of the Debye approximation for gold is justified since it has been experimentally demonstrated that in the metals the Debye approximation is valid up to twice the Debye temperature ($\Theta_D^{bulk} = 165K$)⁽⁵⁹⁾. The two expressions in square brackets of relation (2) are due to the total and to the correlated motion respectively. It has been demonstrated⁽⁵⁸⁾ that for an fcc metal the correlated motion is about 0.35 times the total motion for $T \geq 0.55\Theta_D$ which is the range of temperature of our interest. So relation (4) can be approximated by:

$$\sigma^2(T) = \sigma_S^2 + 0.65 \frac{6\hbar^2}{mk_B\Theta_D} \left[\frac{1}{4} + \left(\frac{T}{\Theta_D} \right)^2 D_1 \right]$$

In Fig. 9 the σ^2 values obtained by extrapolating the straight line to $T=0$ are due to the statical (σ_S^2) and dynamical ($0.98h^2/mk\Theta_D$) factors while the slopes are only due to the dynamical disorder. In Table IV we report the values of the cluster Debye temperatures as deduced from slopes.

TABLE IV - Clusters Debye temperature (Θ_D) and statistical disorder factors (σ_S^2).

$D(\text{\AA})$	$\Theta_D(K)$	$\sigma_S^2(\text{\AA}^2)$
42.5	150	0.80×10^{-3}
30.0	148	0.95×10^{-3}
24.0	148	2.55×10^{-3}
20.0	140	3.80×10^{-3}

The decrease in cluster Debye temperatures are again due to the great number of surface atoms. LEED measurements indeed have shown higher surface atoms mobility with respect to the bulk one and determined surfaces Debye temperatures for different Miller planes⁽⁶⁰⁾. Such Debye temperatures are always lower than the bulk one. In first instance we supposed that the cluster Debye temperatures appoache the surface one, averaged on all the possible surfaces, as the cluster size decreases. This average, using literature data⁽⁶⁰⁾, gives for gold:

$$\Theta_D^{cluster} = 135K \approx 0.8\Theta_D^{bulk}$$

that is in good agreement with data of Table IV.

To evaluate the statical disorder we subtracted from $T^2=0$ cluster σ^2 values obtained from Fig. 9, the dynamical contribution given by

$$\frac{0.98h^2}{mk\Theta_D^{cluster}}$$

Table IV reports the σ_S^2 values obtained. The increase in statical disorder is only partially due to the cluster size distribution inside each sample. In fact for a film, containing clusters of 20\AA , using the values of Tables. I and II for the cluster size distributions and the nn distance values respectively,

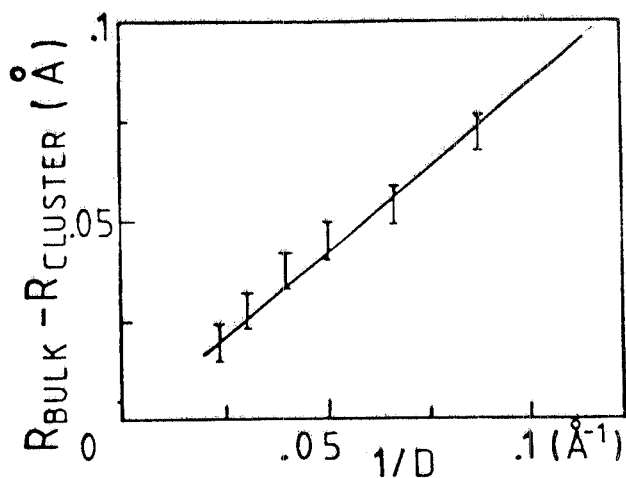


FIG. 7 - Plot of nearest neighbour distance contraction vs. the inverse of the cluster mean diameter. The straight line drawn is the data mean square linear fit.

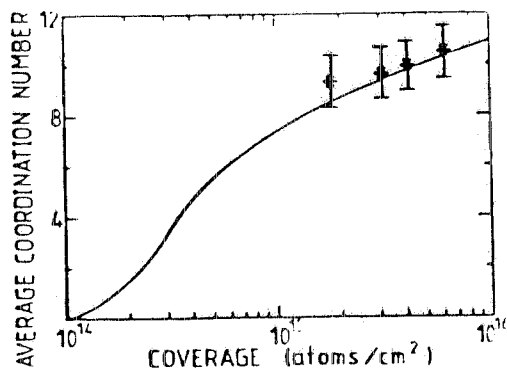


FIG. 8 - Behaviour of the average coordination number versus coverage for gold on carbon (solid line) (Ref(1)). The stars (*) are experimental data obtained for our gold clusters on mylar.

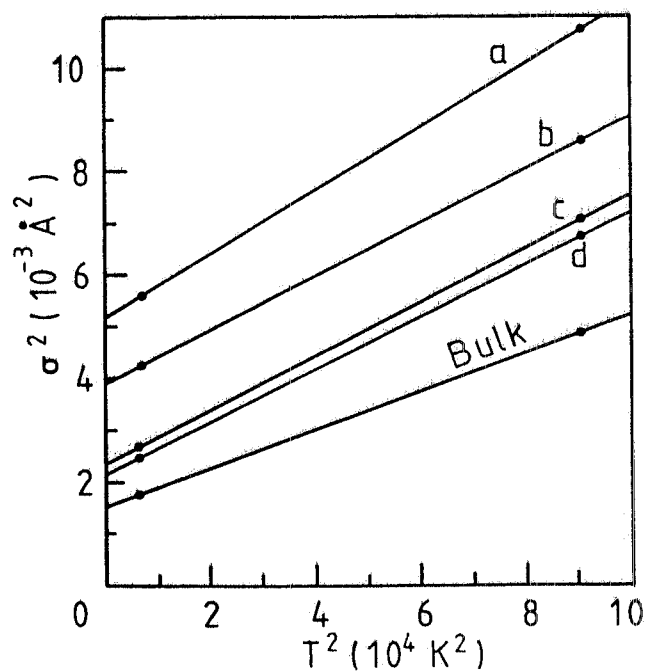


FIG. 9 - Plot of the Debye-Waller factor vs. T^2 for some of the samples studied: a) 20 Å clusters, b) 24 Å clusters, c) 30 Å clusters and d) 42.5 Å clusters. The bulk σ_B^2 at 77 K has been assumed equal to $1.7 \times 10^{-3} \text{Å}^2$, according to Ref. (59).

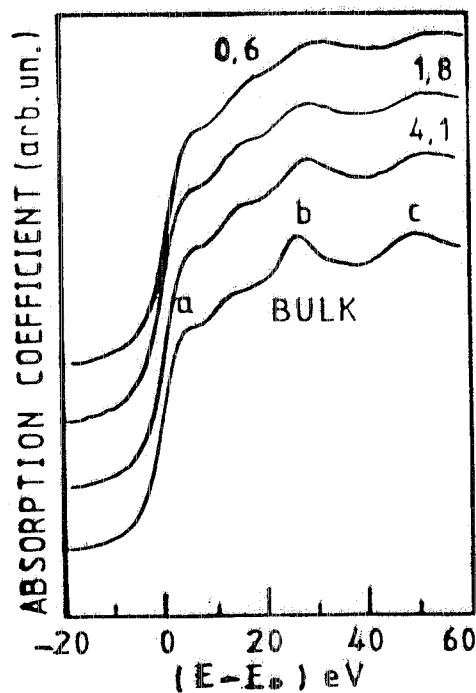


FIG. 10 - XANES spectra for some of the samples studied. Coverages indicated are in units of $10^{15} \text{atoms/cm}^2$; the zero of the energy has been assumed at the edge inflection point.

we calculated a static disorder factor of 10^{-3} \AA^2 that is smaller than the value reported in Table IV.

Moreover the slight static disorder found, cannot be ascribed to structural changes to icosahedra. This agrees with thermodynamical considerations that predict a structural transition from fcc to icosahedra for clusters containing less than 150 atoms^(31,61-62). In the icosahedra indeed the first fcc shell is splitted in two shells centered at distances R_I and R_{II} related by

$$R_I = 1.05R_{II}.$$

Such system would have a $\sigma_S^2=0.012 \text{ \AA}^2$ much greater than the values observed.

In order to completely exclude the presence of icosahedral structure in our samples, we performed fits of the inverse Fourier transform spectra, using a fcc model and an icosahedric model. Only using a single shell fcc model, we obtained good fits for all samples.

The question if the structure is still fcc up to the second and third shell, can be fully clarified from the XANES spectra^(35,36), shown in Fig. 10, which have a typical fcc shape in going from the bulk to the 11 Å cluster. The two peaks labelled b and c indeed have been proved to come out only in fcc structures ordered up to the third shell⁽⁶⁴⁾. It can be seen that as the cluster size decreases there is a shift to higher energies and a broadening of the XANES peaks. The former is due to the shortening of the lattice parameters⁽⁶⁵⁾, while the latter is a consequence of both the cluster size distribution inside each sample and of the different weight of the second and third shell contributions to the spectra for different samples. A quantitative analysis of the XANES data will be published elsewhere.

5. - CONCLUSIONS

In conclusion we have shown that in Au evaporated metal clusters on a weakly interacting substrate the cluster structure is still fcc, like the bulk one, but there is a contraction of the nn distance. We quantitatively determined this contraction for cluster sizes ranging from 11 Å up to 60 Å.

We measured the rms deviations of atoms around their positions and found that they are mainly dynamical in character. We deduced the Debye temperatures of the cluster studied which were in excellent agreement with LEED data.

Nonetheless, it is our opinion that a lot of things must be solved, in particular in the cluster-substrate interaction, in order to achieve a general consistent picture of small cluster behaviour and to understand the discrepancies existing in literature.

ACKNOWLEDGMENTS

The authors are grateful to LNF machine staff and to the Synchrotron Radiation group for their collaboration during measurements. Thanks are due to Dr. P. Rosa for the electron microscopy analysis, performed at the Istituto Superiore di Sanita' of Rome. The fruitful discussions with Dr. L. Incoccia have been invaluable during all stages of this work.

References

- ¹M. G. Mason, Phys. Rev. B 27, 748 (1983).
- ²M. G. Mason, L. J. Gerenser and S. T. Lee, Phys. Rev. Lett. 39, 288 (1977).
- ³R. C. Baetzold, J. Chem. Phys. 68, 555 (1978).
- ⁴J. Colbert, A. Zangwill, Myron Strongin, S. Krummacher, Phys. Rev. B 27, 1378 (1983).
- ⁵C. Battistoni, G. Mattogno, R. Zanoni and L. Naldini, J. Electron Spectrosc. 28, 23 (1982).
- ⁶K. S. Liang, W. R. Salamek, I. A. Aksay, Solid State Commun. 19, 329 (1976).
- ⁷G. O. Ozin and F. Hugues, J. Phys. Chem. 87, 94 (1983).
- ⁸R. C. Baetzold, M. G. Mason and J. H. Hamilton, J. Chem. Phys. 72, 366 (1980).
- ⁹W. F. Egelhoff Jr. and G. G. Tibbets, Phys. Rev. B 19, 5028 (1979).
- ¹⁰H. Roulet, J. M. Mariot, G. Dufour and C. F. Hague, J. Phys. F. 10, 1025 (1980).
- ¹¹S. R. Sashital, J. B. Cohen, R. L. Burwell Jr. and J. B. Butt, J. Catal. 50, 479 (1977).
- ¹²J. H. Sinfelt, G. H. Via, F. W. Lytle and R. B. Gregor, J. Chem. Phys. 75, 5527 (1981).
- ¹³J. H. Sinfelt, G. H. Via, F. W. Lytle, J. Chem. Phys. 76, 2779 (1982).
- ¹⁴G. H. Via, J. H. Sinfelt, F. W. Lytle, J. Chem. Phys. 71, 690 (1979).
- ¹⁵G. Apai, J. Hamilton, J. Stohr and A. Thompson, Phys. Rev. Lett. 43, 165 (1979).
- ¹⁶H. Purdum, P. A. Montano, G. K. Shenoy and T. Morrison, Phys. Rev. B 25, 4412 (1982).
- ¹⁷J. Sinfelt, Rev. Mod. Phys. 51, 569 (1979).
- ¹⁸J. Q. Broughton and L. V. Woocook, J. Phys. C.: Sol. St. 11, 2743 (1978).
- ¹⁹J. L. Dormann, Rev. Phys. Appl. 16, 275 (1981).

- ²⁰J. L. Dormann , D. Fiorani, J. L. Tholence and C. Sella, , J. Magn. Magn. Mater. 35, 117 (1983).
- ²¹W. F. Egelhoff Jr. and G. G. Tibbetts, Phys. Rev. B 19, 5028 (1979).
- ²²J. F. Hamilton and P. C. Logel, Thin Solid Films 16, 49 (1973).
- ²³J. F. Hamilton and P. C. Logel, Thin Solid Films 23, 89 (1974).
- ²⁴M. De Crescenzi et al., Solid State Commun. to be published .
- ²⁵M. Boudart et al., J. Catal. 6, 92 (1966).
- ²⁶W. F. Taylor, D. J. C. Yates and J. H. Sinfelt, J. Am. Chem. Soc. 86, 2966 (1964).
- ²⁷P. Schoubye, J. Catal. 14, 238 (1969).
- ²⁸C. Berry, Phys. Rev. B 88, 596 (1952).
- ²⁹H. J. Wasserman and J. S. Vermaack, Surf. Sci. 22, 164 (1970).
- ³⁰C. L. Briant and J. J. Burton, Surf. Sci. 51, 345 (1975).
- ³¹M. B. Gordon, F. Cyrot-Lackmann and M. C. Desjonqueres, Surf. Sci. 80, 159 (1980).
- ³²B. Moraweck and A. J. Renouprez, Surf. Sci. 106, 35 (1981).
- ³³P. A. Lee , P. H. Citrin, P. Eisenberger and B. M. Kincaid, Rev. Mod. Phys. 53, 769 (1981).
- ³⁴E. A. Stern, D. E. Sayers and F. W. Lytle, Phys. Rev. B 11, 4836 (1975).
- ³⁵M. Belli et al., Solid State Commun. 35, 355 (1981).
- ³⁶J. B. Pendry in "EXAFS and Near Edge Structure " - A. Bianconi, L. Incoccia, S. Stipcich editors, Springer Verlag 1983 pag.4 .
- ³⁷J. P. Marton and J. R. Lemon, Phys. Rev. B 4, 271 (1971).
- ³⁸S. Normann, T. Andersson, C. G. Granqvist and O. Hundery, Phys. Rev. B 18, 674 (1978).
- ³⁹R. Barbini et al., Riv. Nuovo Cim. 4 (1981).
- ⁴⁰E. Burattini et al., Nucl. Instr. Meth. 208, 91 (1983).
- ⁴¹S. Mobilio, F. Comin and L. Incoccia, LNF internal report 82/19 (NT) (1982).
- ⁴²F. W. Lytle, D. E. Sayers and E. A. Stern, Phys. Rev. B 15, 2426 (1977).

- ⁴³B. K. Teo and P. A. Lee, *J. Am. Chem. Soc.* 101, 2815 (1979).
- ⁴⁴P. Rabe, G. Tolkien and A. Werner, *J. Phys. C :Sol. St. Phys.* 12, 899 (1979).
- ⁴⁵P. H. Citrin, P. Eisenberger and B. M. Kincaid, *Phys. Rev. Lett.* 36, 1346 (1976).
- ⁴⁶E. A. Stern, B. A. Bunker and S. M. Heald, *Phys. Rev. B* 21, 5521 (1980).
- ⁴⁷D. E. Sayers, E. A. Stern and F. W. Lytle, *Phys. Rev. Lett.* 35, 584 (1975).
- ⁴⁸G. Martens , P. Rabe, N. Schwentner and A. Werner, *Phys. Rev. B* 17, 1481 (1978).
- ⁴⁹P. Rabe, *Jap. J. Appl. Phys.* 17, 22 (1978).
- ⁵⁰P. Eisenberger and G. S. Brown, *Solid State Commun.* 29, 481 (1979).
- ⁵¹R. Heansel et al., in "Proc. NATO Adv. Study Inst.:Liquid and Amorphous Metals" E. Luscher editor (D. Reidel, Dodrech ,1980).
- ⁵²M. De Crescenzi et al., *Sol. St. Commun.* 37, 921 (1981).
- ⁵³S. Mobilio and L. Incoccia, to be published on *Nuovo Cimento*.
- ⁵⁴E. C. Marqués , D. R. Sandstrom, F. W. Lytle and R. B. Gregor, *J. Chem. Phys.* 77, 1027 (1982).
- ⁵⁵C. W. Mays, J. S. Vermaak and D. Kuhlmann-Wilsdorf, *Surf. Sci.* 12, 134 (1968).
- ⁵⁶P. Lagarde et al., *J. Catal.* 84, 333 (1983).
- ⁵⁷P. A. Montano and G. K. Shenoy, *Solid State Commun.* 35, 53 (1980).
- ⁵⁸G. Beni and P. M. Platzmann, *Phys. Rev. B* 14, 9514 (1976).
- ⁵⁹R. B. Gregor and F. W. Lytle, *Phys. Rev. B* 20, 4902 (1979) ; E. Sevillano, H. Meuth and J. J. Rehr, *Phys. Rev. B* 20, 4908 (1979).
- ⁶⁰D. P. Jackson, *Surf. Sci.* 43, 431 (1974).
- ⁶¹J. P. Borel, *Surf. Sci.* 106, 1 (1981).
- ⁶²J. J. Burton, *Cat. Rev. -Sci. Eng.* 9, 209 (1974).
- ⁶³The Cernlib Minuit program has been used for least mean square fitting.
- ⁶⁴G. N. Greaves , P. G. Durham, G. Diakun and P. Quin, *Nature* 294, 139 (1981).
- ⁶⁵C. R. Natoli ,in " EXAFS and Near Edge Structure "- A. Bianconi, L. Incoccia, S. Stipcich editors, Springer Verlag 1983 pag.43 .